



Atomic force microscopy of biological samples

David P. Allison^{1,3}, Ninell P. Mortensen¹, Claretta J. Sullivan², and Mitchel J. Doktycz^{1*}

The ability to evaluate structural–functional relationships in real time has allowed scanning probe microscopy (SPM) to assume a prominent role in post genomic biological research. In this mini-review, we highlight the development of imaging and ancillary techniques that have allowed SPM to permeate many key areas of contemporary research. We begin by examining the invention of the scanning tunneling microscope (STM) by Binnig and Rohrer in 1982 and discuss how it served to team biologists with physicists to integrate high-resolution microscopy into biological science. We point to the problems of imaging nonconductive biological samples with the STM and relate how this led to the evolution of the atomic force microscope (AFM) developed by Binnig, Quate, and Gerber, in 1986. Commercialization in the late 1980s established SPM as a powerful research tool in the biological research community. Contact mode AFM imaging was soon complemented by the development of non-contact imaging modes. These non-contact modes eventually became the primary focus for further new applications including the development of fast scanning methods. The extreme sensitivity of the AFM cantilever was recognized and has been developed into applications for measuring forces required for indenting biological surfaces and breaking bonds between biomolecules. Further functional augmentation to the cantilever tip allowed development of new and emerging techniques including scanning ion-conductance microscopy (SICM), scanning electrochemical microscope (SECM), Kelvin force microscopy (KFM) and scanning near field ultrasonic holography (SNFUH). © 2010 John Wiley & Sons, Inc. *WIREs Nanomed Nanobiotechnol* 2010 2 618–634

INTRODUCTION

Gerd Binnig and Heinrich Rohrer published the first images taken with a scanning probe microscope (SPM) in 1982.¹ Their new invention, the scanning tunneling microscope (STM), was able to resolve atomic structure by raster scanning a sharp, conductive tip over a conductive sample. The obvious implications of this high-resolution microscope capable of imaging in air was not lost on biologists who quickly teamed with physicists to develop techniques for imaging biological samples

including DNA,^{2–8} proteins,^{9–14} viruses^{15,16} and components of bacterial surfaces.¹² Although STM was used to image biomolecules, images were difficult to reproduce and not necessarily representative of the biological system of interest due to the need for a conductive sample. Nevertheless, the STM was responsible for establishing a fresh new focus on microscopy and marked the development of a new family of SPMs. The most popular member of this family, with regard to biological research, is the atomic force microscope (AFM). This instrument was first described in 1986¹⁷ and became commercially available in 1989. The AFM is related to the STM, but, instead of using a conductive probe to electronically map a surface, a sharpened tip mounted on the end of a flexible cantilever is used (Figure 1). The first instruments imaged in contact mode by monitoring the deflection of the cantilever caused by the interactions between the tip and the sample

*Correspondence to: doktyczmj@ornl.gov

¹Biosciences Division, Oak Ridge National Laboratory, P.O. Box 2008, TN 37831-6445, USA

²Department of Surgery, Eastern Virginia Medical School, P.O. Box 1980, Norfolk, VA 23501, USA

³Department of Biochemistry and Cellular and Molecular Biology, University of Tennessee, Knoxville, TN 37996-0840, USA

DOI: 10.1002/wnan.104

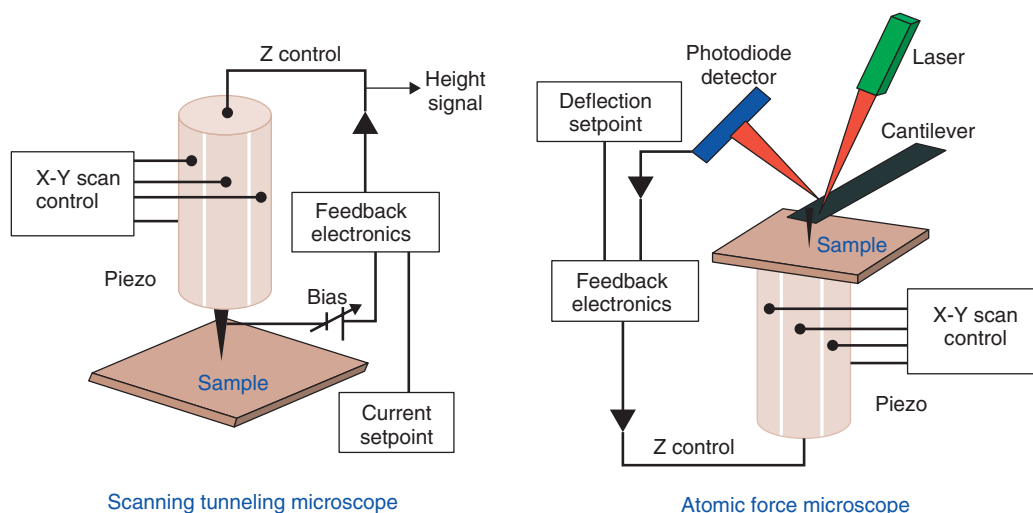


FIGURE 1 | The scanning tunneling microscope (STM) and the atomic force microscope (AFM) differ primarily in the manner in which they sense proximity to the surface. The STM senses changes in surface topography electronically by monitoring a tunneling current, between a conductive tip and a conductive sample, as the surface is scanned. The AFM senses the surface by contacting or near contacting a surface with a sharp tip on the end of a microcantilever. With AFM, height information is gained by reflecting a laser beam off the back surface of the cantilever onto a photodiode. As the sample is scanned, feedback electronics raises or lowers the tip, in response to changes in surface topography, to maintain a constant position where the laser strikes the photodiode. The voltages applied to raise or lower the tip serve as the height input for the image. Both instruments use the same control electronics so that only the surface sensing device is different. This allows for the instrument to be operated as either an STM or AFM.

during scanning.¹⁷ This interaction with the sample created a significant amount of lateral force and in many cases required immobilization techniques for holding biological samples to surfaces.^{18–21} Later, two types of intermittent contact imaging modes were developed, acoustic drive²² and magnetic ac mode^{23,24} in which the cantilever tip is oscillated at its resonance frequency. During scanning, the oscillating tip is brought proximal to the sample surface. Interactions between the tip and the surface dampen the oscillation thereby identifying the surface. As the AFM did not require conducting materials for imaging, images of proteins,^{25–28} DNA,^{18–21,29} and even whole living cells^{30,31} quickly appeared in the literature as scientists embraced this new instrument.

There are advantages and disadvantages for using AFM over conventional microscopes for biological imaging (see Table 1). Since staining, labeling or coating of samples is not required for AFM imaging, direct imaging of biological structures with minimal pretreatment is a significant advantage. Importantly, the AFM can then present these images in a three-dimensional format. By far the greatest advantage of AFM is that cells and biomolecules can be imaged in physiologically relevant environments. In solutions at controlled temperatures, live cell imaging is possible, allowing for dynamic biological events to be studied, at the nanoscale, in real time. Although emerging optical and scanning electron microscopy (SEM) techniques allow structural investigations of

biological systems at the nanoscale in physiological environments, the range of imaging techniques available for AFM allow a far more detailed investigation of functional properties. The time required to record an AFM image previously prevented the capture of biological reactions and events that happen in fractions of seconds. However, commercially available fast-scanning AFMs are beginning to address the need for better temporal resolution. Another perceived disadvantage of conventional AFM includes its restriction to imaging the sample surface, which unlike optical and transmission electron microscopes can look inside cells. Again, emerging techniques such as scanning near field ultrasonic holography (SNFUH) are being developed to overcome this limitation. One limitation of conventional AFM that has yet to be addressed is the limited scan range, in both 2D and height. Typically, scanners are limited to roughly $100 \times 100 \mu\text{m}$ in X and Y and most importantly are restricted to around $10 \mu\text{m}$ for most AFMs in the vertical dimension.

The objective of this review is not to offer a comprehensive description of either AFM instrumentation or applications. A number of excellent review articles and books serve this purpose.^{38–47} Instead, we focus on the application of the AFM to the study of biological systems. Unraveling biological systems requires experimental techniques that can identify, localize, and quantify interactions between component molecules. New and improved instruments continue to address new research challenges. Improved

TABLE 1 | Biological Imaging Techniques

Microscopy	Resolution Limit	Specific Features and Characteristics
Light microscopy	~0.2 μm	Samples can be imaged in liquid or air. Resolution is limited by the wavelength of visible light
Fluorescence microscopy	~0.2 μm	Samples can be imaged in liquid or air. Fluorescence labeling is a well-developed technique that can be used to localize molecular components. Confocal scanning microscopy further enables three-dimensional studies of biological objects. Resolution is traditionally limited by the wavelength of light although super resolution techniques that break the optical resolution barrier are becoming available ^{32–35}
Scanning electron microscopy (SEM)	Nanometer level	For SEM imaging, the sample is placed in a vacuum. Sample coating may be needed, as the technique generally requires an electron conductive sample. The electron beam is used to probe the surface and techniques for heavy metal labeling of surface molecules are often used
Transmission electron microscopy (TEM)	Nanometer level	Image contrast depends on impeding electrons as they pass through the sample, usually by heavy metal staining. Operates under vacuum with resolution depending primarily on image contrast through staining. New advances allow imaging samples in a liquid cell ^{36,37}
Atomic force microscopy (AFM)	Nanometer level	Imaging is accomplished by monitoring the position of a sharpened tip attached to a micro-cantilever as it is scanned over a sample surface. Samples can be imaged in liquid or air with nanometer resolution at atmospheric pressure enabling dynamic studies. AFM provides 3-dimensional surface visualization and measurement of nanomechanical properties of the sample

SPM imaging techniques and other ancillary techniques developed within the SPM platform can assume a benchmark role in the post-genomics era by providing linkages between structure and function and by offering new approaches to biomolecule screening. In this short review, we cannot begin to cover all who have contributed to this development and for this we apologize to the many contributors that have advanced the development of SPM.

LIVE CELL IMAGING

The first image of a live cell, a plant cell, imaged in water appeared in the literature in the early 1990s.⁴⁸ There was a general concern that the delicate cell membrane of living cells would not withstand imaging by AFM and that the cell membrane would rupture due to the forces exerted by the cantilever tip. This fear was unfounded as a number of laboratories soon published contact mode images of a variety of living mammalian cells.^{30,31,49–54} Most of the early work on AFM imaging of cells focused on the imaging of mammalian cells. This is in part due to the fact that mammalian cells generally adhere well to surfaces they are growing on and therefore are not removed by forces exerted by the scanning tip. Conversely, smaller bacterial and yeast cells require immobilization on surfaces before imaging via AFM. Various techniques,

involving entrapment in membrane filters^{55–60} or tethering via surface modifications^{61–67} have been developed to facilitate imaging of microbial cells (Figure 2).

Contact mode AFM imaging with vertical forces on the order 10–30 nN typically do not damage the cell, though these forces are sufficiently high to push the pliable membranes into taut underlying structures, making them visible. The fact that the cytoskeleton network could be observed by AFM was initially a surprise. It is routinely observed that the cell membrane conforms to the rigid cytoskeleton when contacted with the cantilever tip at scanning forces of 2–20 nN.³⁰ By applying a force of 100 nN, a hole could be punched through the cell membrane without apparent damage to the cell.³⁰ Subsequent research on mammalian cells indicates that tip forces depress the membrane to allow imaging of the cell nucleus and the actin network. Imaging Madin–Darby canine kidney (MDCK) cells in liquid, Hoh and Schoenenberger observed that the outline of the cell nucleus could be clearly imaged by increasing the imaging force on the cell even to the point of moving the nucleus without rupturing the cell.^{52,68} Although structures beneath the cell membrane could be imaged by AFM there was a marked absence of these structures when imaged by SEM. It was also determined that, fixing the cell with glutaraldehyde caused the membrane to harden so that

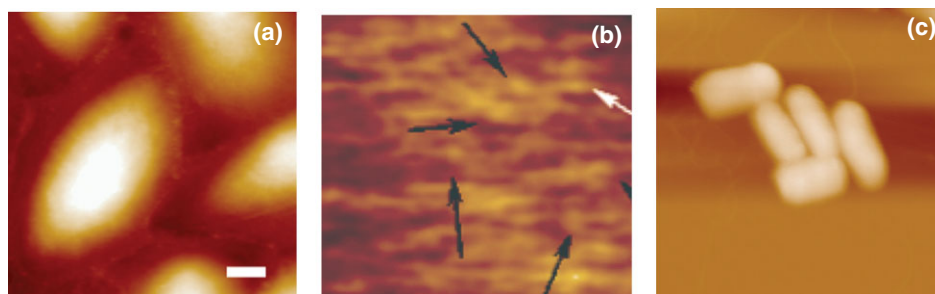


FIGURE 2 | AFM images of African green monkey kidney cells (CV-1) taken in contact mode using a Nanoscope III atomic force microscope (AFM) (Veeco Instruments, Santa Barbara, CA). In Image (a) the scale bar is 10 μm with a Z range of 8 μm . By adjusting the scanning force to 20–50 pN high-resolution images (b) of the cell surface reveal globular structures (black arrows) and elongated particles (white arrow) with lateral diameters of ~ 20 nm with heights of ~ 10 nm. The CV-1 images were kindly provided by Dr. Christian LeGrimellec, INSERM/UNIV-MONTP 1/CNRS, Montpellier, France. The (c) image taken in contact mode, on a PicoPlus AFM (Molecular Imaging, Tempe, AZ), shows several *E. coli* bacteria mounted on a gelatin surface and imaged in water.⁶⁷

the outline of the nucleus could not be seen by AFM. In contrast to the nucleus, microvilli that cover the surface of the MDCK cells were clearly seen by SEM but were absent when imaged by AFM.⁵² When cells were fixed, their surfaces became markedly rough, potentially due to the stabilization of the microvilli, allowing these structures to be imaged by AFM. The results obtained from imaging mammalian cells in contact mode, where typical forces of 2–20 nN are exerted on cells, raises two important questions.

The first question concerns the quality and reliability of images that result when imaging with applied forces that deform the plasma membrane to the extent reported. Hoh and Shoenenberger,⁵² using force curve measurements on MDCK cells, calculated that contact with the apical cell membrane, which caused the cantilever to deflect 35 nm, caused the cell membrane to be pushed in approximately 1000 nm. This translates into the cell membrane having a spring constant of 0.002 N/m, which is less than 1/10 of the cantilever spring constant of 0.06 N/m. This finding is very close to what Weisenhorn et al. reported on a lung cancer cell line where a force of 1–10 pN resulted in a 1 nm deformation in the plasma membrane.⁶⁹ When the tip is pressing into the cell there is a greater area of contact between the tip and surface and therefore the resolution is adversely affected.^{53,70,71} Using silicon nitride cantilevers with measured spring constants of either 0.01 or 0.03 N/m, LeGrimellec et al. found that the engagement force before any adjustments were made using contact mode AFM was between 5 and 15 nN. This force, exerted on a sample of cultured CV-1 African green monkey kidney cells, resulted in the removal of the cells from the mounting surface. By measuring force curves prior to imaging, the engaged tip was retracted incrementally from the surface until forces less than 100 pN, and often in the range of

20–50 pN, were obtained with tip indentation of the surface generally in the 10 nm range. This allowed routine imaging of these cells with lateral resolution of better than 20 nm and occasionally 10 nm resolution (Figure 2). Low-resolution images showed a smooth surface with very little indication of the submembrane cytoskeleton. Higher resolution images revealed a more granular surface packed with particles that were likely proteins or protein–lipid complexes.⁷² Unlike green monkey kidney cells, MDCK are rich in microvilli. The surface of these cells, imaged in contact mode with scanning forces of 2 nN and above, shows a smooth surface. However, by decreasing the force to less than 300 pN microvilli are prominently displayed.⁷³ These experiments establish that by reducing the imaging force on cells the magnitude of indentation of the cell surface is reduced resulting in improved resolution.

The second question concerns the effect that such forces might have on the vitality of the cell being imaged. By increasing the force of the cantilever on the cell surface, holes are created in the cell that repair over a period of time.³⁰ Glial cells have been manipulated with the AFM cantilever and even had cellular processes severed without killing the cells.⁷⁴ However, the question is still open as to what effect both normal and extreme imaging conditions have on the overall metabolic activity of cells. Instrument induced changes by applied scanning forces of 1–5 nN are hard to separate from normal intracellular cytoskeletal changes and other biological reactions and cellular processes that may be promoted or inhibited by the AFM tip. Living cells are also generally imaged at room temperature in a buffer rather than growth media. By returning cells to growth media after AFM imaging, depending on the cell type, cells have remained viable for at least 24 h.^{68,75}

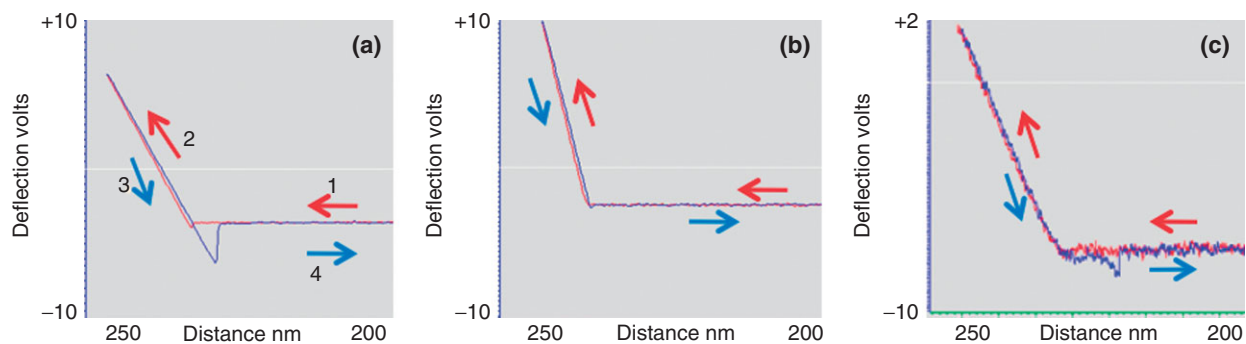


FIGURE 3 | Sensing forces with the atomic force microscope (AFM) cantilever is a non-imaging application of AFM. As shown in (a), the number 1 position on the figure shows that the cantilever is not yet on the surface but moving toward the surface (red arrow). The red line on the force curve is the approach while the blue line is the retraction of the cantilever. As the cantilever touches the surface it begins to deflect, as indicated by position 2. This serves as the signal for the cantilever to retract, position number 3 (blue arrow). When force curves are done in air there is a water bridge that can form between the cantilever tip and the surface that causes an adhesion event requiring force to break this contact, as the cantilever tip abruptly jumps off the surface (position number 4). By knowing the spring constant of the cantilever and determining the slope of the cantilever deflection, one can calculate the spring constant of the surface. In (b), the same process was repeated in water, notice that the water bridge between the cantilever tip and surface does not form and therefore no adhesion event. In (c), a specific probe (biotin) is attached to the cantilever tip, by a polyethylene glycol tether, while the surface is covered with avidin. In a liquid environment the tip approaches the surface makes contact, is retracted, moves off the surface, and an adhesion event occurs due to the biotin/avidin interaction. The force required to break this interaction can also be calculated and since the biotin is tethered to the cantilever the adhesion event will occur at approximately the length of the tether.

The application of intermittent or non-contact imaging modes, known in the literature as ‘tapping mode’²² or ‘MacMode’,^{23,24} should prove valuable for looking at cell surfaces. In these modes, where the cantilever is oscillated at its resonant frequency, dampening of the oscillation amplitude as the tip nears the surface is used to register the surface. Because the tip only makes intermittent contact with the surface, the problems caused by tip deformation that result in loss of resolution is minimized.^{76–79} Imaging in either of these two modes also reduces the lateral forces applied to the sample, by the tip during scanning, thereby minimizing removal of samples that are not well immobilized on surfaces.

FORCE MEASUREMENTS

Although the AFM was designed primarily as an imaging tool, the sensitivity of the AFM cantilever to forces has been developed into a unique and separate application. Measuring the interaction between the cantilever tip and a glass surface in water, Paul Hansma’s group detected adhesive interaction forces that they attributed to either the rupture of individual hydrogen bonds or interaction with ordered water layers near the surface.⁸⁰ Since this early report, a significant amount of research effort has been devoted to using the AFM cantilever as a force sensing device in biological research. Perhaps in its simplest form, the AFM cantilever has been used to measure forces by engaging the cantilever tip with the cell surface

and pushing on the surface to acquire a force distance curve (Figure 3). By knowing the dimensions of the tip and the spring constant of the cantilever, the stiffness of the cell can be calculated. Vinculin is one of the intracellular membrane adhesion proteins that bind the cell membrane to the cytoskeleton. Using a mouse F9 embryonic carcinoma cell line that was vinculin deficient, Goldmann et al. performed elasticity experiments by AFM to determine the spring constant of the cell surface using force distance curves. They found that a vinculin mutant was 21% less stiff than the same cell line after transfection with a plasmid that produced vinculin.⁸¹

The cell surface elasticity of bacterial cell surfaces has also been determined after exposure to various environmental conditions. For example, the effect of the antimicrobial peptide colistin, on *Pseudomonas aeruginosa*, a prominent cause of lung infections in patients with cystic fibrosis has been reported. In this study after 2 h of colistin treatment, at concentrations not sufficient to cause cell death, a significant increase in the bacterial spring constant, compared to untreated bacteria, was observed.⁶² There is an extensive body of work that describes AFM methods for measuring the rigidity of both bacterial^{62,63,82–89} and mammalian cells.^{52,81,90–97}

The extreme mechanical sensitivity of the cantilever can be exploited to measure forces both within and between biomolecules. Forces required to rupture bonds between complementary oligonucleotides have been accomplished by attaching one single-stranded

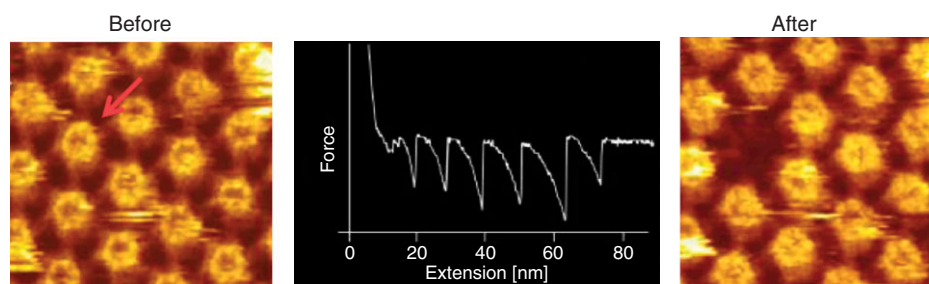


FIGURE 4 | The first atomic force microscope (AFM) image shows an isolated cell membrane from *Deinococcus radiodurans* with pores structures. As the cantilever tip is brought in contact with the surface and retracted the force-extension curve shows six force peaks, of about 300 pN each, required to extract all six protomers of a single bacterial pore from the surface. The distance between each of the protomer disruption events is 7.3 nm. The second image of the same surface shows that an entire bacterial pore was extracted from the surface. (Reprinted with permission from Ref 109. Copyright 1999 National Academy of Sciences, USA).

DNA molecule to the cantilever tip and its complement to the surface.^{98,99} Experiments similar to these have been done by attaching biotin to the cantilever and either avidin^{100,101} or streptavidin¹⁰² to the surface. During retraction of the tip from the surface, the force required to pull the interacting molecules apart can be measured (Figure 3). Another report describes attaching a single eukaryotic cell to the cantilever and interacting it with another cell growing in a petri dish and measuring the force required to break the bond of the adhesion protein CsA between cells.¹⁰³ The forces reported to rupture interactions between molecules depend on the force loading rate. Results can be reasonably consistent when reported by different laboratories. For example, when a gold coated tip and a gold coated surface were modified with 11-mercaptoundecanoic acid by reacting the thiol groups with the gold and allowing the carboxylic acid groups to interact, the force required to break a single hydrogen bond was found to be 16.6 pN.¹⁰⁴ In a similar experiment, from a different laboratory, where hydrogen bonds were allowed to interact, the rupture force was found to be 12 pN.⁸⁰

A force extension curve is generated by approaching a surface with the cantilever tip, touching biomolecules immobilized on the surface with the tip, and retracting the tip. If a biomolecule becomes attached to the tip, the distance traveled to retract the tip from the surface and the forces required to extend the biomolecule can be determined. In the literature this type of analysis is often called either dynamic force microscopy (DFM) or dynamic force spectroscopy (DFS). The mechanical proteins titin^{105–107} and tenascin¹⁰⁸ have been extensively studied with this type of single molecule force spectroscopy. For titin, reported maximum force peaks varied between 150 and 300 pN with a periodicity of 25–28 nm. The expected distance to unravel a single titin Ig domain is 31 nm.¹⁰⁵ Results from other experiments of this

type are shown in Figure 4 where Müller et al. demonstrated the unzipping of an entire bacterial pore from an isolated membrane surface of *Deinococcus radiodurans*. All six of the protomers in the pore could be extracted with an average force of 300 pN required for each of the protomers and with an average distance of the disruption event between protomers being 7.3 nm.¹⁰⁹ In addition to proteins, AFM force spectroscopy experiments have been performed on polysaccharides¹¹⁰ DNA¹⁰⁵ and alcohols.¹¹¹

Receptor-ligand binding has been investigated on whole cells using functionalized tips in a liquid environment. In these experiments, antibodies, lectins, and other biomolecules that specifically interact with receptors on cell surfaces are tethered to the cantilever tip through a linker molecule that is usually 2–10 nm in length.¹¹² During the approach, the tethered molecule has an opportunity to bind its complement on the cell surface. Upon retraction, if binding has occurred, the unbinding force is recorded as a sudden change in force just as the tethered molecule disengages and the cantilever returns to its baseline position. This unbinding force can be distinguished from nonspecific binding by a specific adhesion interaction occurring at roughly the distance of the linker from the point where the cantilever first contacts the surface (Figure 3C). Gad et al. used gold thiol chemistry to functionalize tips with concavalin A, a lectin which recognizes mannose receptors on yeast cell surfaces. They obtained force curves and could resolve forces of 100–500 pN that indicated specific interactions with the mannose receptors. To determine that specific reactions between mannose and concavalin A had been recorded, free mannose was added to block access of tip-associated concavalin to surface mannose. Under this condition, they did not identify adhesion events.¹¹³ In a similar study, Grandbois et al. used this AFM technique to type red blood cells by probing a mixed monolayer of A and O

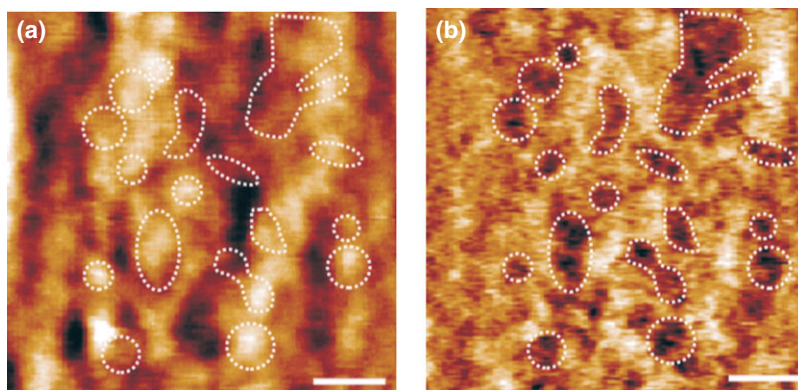


FIGURE 5 | Simultaneous recorded atomic force microscope (AFM) images (A) topography and (B) recognition (TREC) on gently fixed MyEnd cells acquired with a fibrinogen-coated AFM tip. In both images the outlined areas identify places where fibrinogen attached to the cantilever interacts with vascular endothelial (VE)-cadherin. The topographic image is not affected by interaction of the fibrinogen on the AFM tip while the recognition image shows dark spots where the interaction between fibrinogen and (VE)-cadherin occurs. This AFM capability, developed by the Hinterdorfer group, separates the minimum and maximum peaks of an oscillating cantilever as it interacts with a sample surface thereby allowing simultaneous acquisition of topographic and recognition images. The minima of the oscillating cantilever wave contributes the topographic information while the maxima is the source of the recognition image. Scale bars on both images are 200 nm. (Images courtesy of Dr. Peter Hinterdorfer, Johannes Kepler University of Linz, Linz, Austria.)

blood cells using a lectin, which binds to glycolipids on Type A erythrocytes. Using force mapping they could differentiate between A and O cells.¹¹⁴ This is another active area of research where attaching a specific probe molecule to the AFM tip can be used to determine interactions with target molecules on surfaces¹¹⁵ including bacterial,^{116,117} yeast^{118,119} or mammalian cell^{112,114,120–124} surfaces.

The concept of imaging and simultaneously localizing recognition events was realized with molecular recognition force microscopy (MRFM) or topography and recognition (TREC) microscopy. Imaging is accomplished in a non-contact mode using an oscillating tip to which a probe molecule is attached through an 8–30 nm polyethylene glycol tether. Images of a surface can be obtained simultaneously with recognition force interactions. This was first demonstrated by Hinterdorfer's group where an antibody to lysozyme was tethered to the cantilever tip. Topographic images were taken in liquid environment as the modified tip was scanned over lysozyme immobilized on a mica surface. The topographic image becomes distorted due to the interaction of the tethered antibody with the lysozyme coated surface. By adding free lysozyme to the imaging solution, the antibody on the tip was blocked and the distorted images of lysozyme returned to undistorted topographic images.¹²⁵ In principle topographic and recognition images of any surface can be acquired simultaneously by separating information gained from the bottom (topography) and top (recognition) of the oscillating cantilever wave as

the surface is scanned. This technology 'TREC' has also been pioneered by the Hinterdorfer group^{122,126} using mouse myocardium (MyEnd) cells and a tip with fibrinogen attached that interacts with (VE)-cadherin on the endothelial cells as shown in Figure 5.

IMAGING DYNAMIC PROCESSES

Perhaps the greatest advantage for using the AFM as an imaging tool for biological research is that samples can be imaged in liquid and therefore observing dynamic processes is possible. The ability to image DNA in liquid environments has led to a number of dynamic studies.^{127,128} By limiting a transcription buffer, containing double-stranded DNA and RNA polymerase, to three nucleotide triphosphates (NTPs) it was possible to stall transcription complexes. In a flow through AFM cell RNA polymerase of the stalled complexes was bound to a mica surface but by adjusting the Zn^{2+} ion concentration DNA was loosely bound so that by adding low concentrations of the four NTP's time lapse movies of DNA passing through RNA polymerase could be documented although the RNA transcripts were too short to be seen.¹²⁹ Radmacher et al. studied the fluctuation of the enzyme lysozyme by absorbing the protein molecules to a mica surface, and placing the AFM cantilever tip on top of a monolayer of lysozyme.¹³⁰ When the tip was over bare mica no height fluctuations were observed, but when the tip was over lysozyme, small fluctuations were present. When an oligoglycoside substrate was added, the fluctuations became more

pronounced and could be eliminated by adding the inhibitor chitobiose. The most logical interpretation of these results would be that the height fluctuations correspond to conformational changes in the enzyme during the hydrolysis of the oligoglycoside. However the authors did not rule out the possibility that the changes in height were due to the transient complex between the enzyme and substrate.¹³⁰ Other dynamic studies have shown that changes in protein shape can be observed by AFM during enzymatic activity.^{71,128,130} In another study Wang et al. showed adenosine triphosphate (ATP) dependent remodeling of mouse mammary tumor virus (MMTV) promoter nucleosomal arrays that had been incubated with the human Swi-Snf remodeling complex (Figure 6). AFM Images of the nucleosome arrays, taken in liquid, clearly demonstrated that changes occurred after ATP was introduced into the wet cell and the same area was imaged again.¹³¹

Dynamic studies have not been confined to biomolecules. Structural changes in mammalian cells, such as the destruction of the actin network in fibroblasts by cytochalasin B have also been documented.¹³² A number of laboratories have followed changes in normal cellular processes.^{30,68,74} Sequential images to show extension and withdrawal of lamellipodia, changes in cell shape, vesicular structures traveling

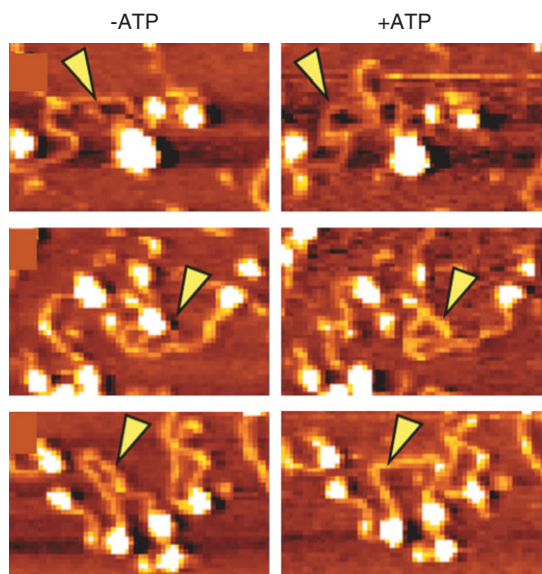


FIGURE 6 | In this study ATP-dependent human Swi-Snf remodeling complex was incubated with mouse mammary tumor virus (MMTV) promoter nucleosomal arrays and deposited on mica surfaces pretreated with aminopropyltriethoxysilane (APTES) activated with glutaraldehyde.¹³¹ In the three AFM images taken before ATP and after ATP was added changes (arrowheads) in the nucleosome complexes are clearly seen. (Images courtesy of Dr. Stuart Lindsay, BioDesign Institute, Arizona State University, Tempe, Arizona.)

along the cytoskeletal fibers, and rippled cytoskeletal rearrangements propagating through cells have been reported.⁶⁸ Another study showed a series of images where platelets were activated by contact with the AFM tip. The normally ovoid shaped platelets were seen to spread out into a flattened shape that resembles a fried egg.⁵³ Also recorded were a sequence of AFM images showing exocytosis of a single pox virus from an infected living monkey kidney cell immobilized on a suction pipette.^{50,133} In another dynamic imaging experiment, Bhanu Jena's laboratory collected AFM images of the apical region of cultured pancreatic acinar cells. They identified pits of 500–2000 nm diameter containing 3–30 depressions measuring 100–180 nm in diameter. Stimulation of the cells with secretagogue Mas7 caused release of the starch digesting enzyme amylase. A time course AFM study showed that the diameter of the depressions correlated with the release of amylase. These results suggested that the depressions were exocytotic fusion pores.¹³⁴ These studies represent only a fraction of dynamic processes that have been recorded by AFM in liquid environment, but demonstrate the power of the AFM for capturing dynamic events.

EMERGING IMAGING TECHNIQUES

As already described, AFM has significantly contributed to life sciences with high-resolution imaging of molecules and cells. Also high fidelity measurements of mechanical properties and physical interactions have been reported. In addition, the capability to record dynamic processes in liquid environment, at high-resolution, is a unique feature of AFM. These well established techniques are continuously augmented with emerging implementations of the AFM. With respect to imaging, high-speed AFM is becoming available and facilitates the study of fast dynamic biological process in real time.¹³⁵ Imaging techniques such as scanning ion-conductance microscopy (SICM),¹³⁶ scanning electrochemical microscope (SECM),¹³⁷ Kelvin force microscopy (KFM)¹³⁸ and SNFUH¹³⁹ are powerful techniques that have been integrated into AFM.

Toshio Ando's laboratory was the first to develop a high-speed AFM by incorporating a high-speed scanning mechanism capable of scanning at 60 kHz and using cantilevers with high resonant frequencies of 450–650 kHz with low spring constants of 150–280 pN/nm. This allowed the capture of 'tapping mode' images of 100 × 100 pixels in 80 ms leading to movies of dynamic processes.¹³⁵ High-speed movies, taken at 100 ms/frame, of purple membranes showing movement of bacteriorhodopsin

trimers¹⁴⁰ and images of human chromosomes have recently been reported.¹⁴¹ Other high-speed imaging systems have also been described from the Hansma¹⁴² and Miles¹⁴³ groups.

A new adaptation of SPM called SICM was first demonstrated by Paul Hansma's laboratory. This new technique used a micropipette that had been pulled from capillary tubing so that only a small aperture (0.05–0.1 μm) existed at the tip. Both the pipette, mounted on a piezoelectric scanner configured to move in the X, Y, Z directions, and a wet cell containing the sample had electrodes installed and were filled with 0.1 M NaCl. By applying a dc voltage to the electrode in the wet cell a dc current was established between the two electrodes. As the tip approaches and nears contact with the surface, ion flow through the tip is partially blocked and there is a decrease in current flow. By applying voltages to the Z piezo to raise or lower the tip, in order to maintain a constant current while the sample is scanned, these voltages serve as height input for the topographic image. Alternatively, the tip can be scanned over a surface at a constant height to measure differences in ion currents coming off the surface.¹³⁶

Another application of SICM involves operating the instrument as an AFM in tapping mode where the oscillation of the quartz pipette was found to vary between 50 and 100 kHz. In this configuration the instrument was operated as a combination of AFM for imaging and SICM for sensing ion current.¹⁴⁴ Further improvement in the application of SICM has allowed for lower forces to be exerted on the specimen during imaging. The Korchev group determined that when SICM is operated with maximum sensitivity, where the position of the probe is very close to the surface and strongly influences ion current, the tip is so close that the sides of the tip will exert excessive force on neighboring structures on the sample. A scanning algorithm, where the set point is adjusted to maintain a tip distance greater than the tip radius, minimized the forces exerted on the sample.¹⁴⁵ In Figure 7 two

unpublished images provided by Dr. Yuri Korchev illustrate the utility of the SICM imaging technique. A recent publication using this technique has reported images of proteins in living cell membranes.¹⁴⁶ An adaptation of the SICM technique called 'hopping mode' allowed non-contact imaging of cultured rat hippocampal neuron cell surfaces with resolution better than 20 nm.¹⁴⁷

The SECM developed by Bard's laboratory is a chemical microscope that is based on mass transfer and electrochemical reactions occurring at the sample surface and scanning tip. SECM experiments can be performed in the so-called generation-collection mode (GC mode), where the solution initially does not contain any electroactive species,¹⁴⁸ or the so-called feedback mode (FB mode), where a redox mediator is added to solution.¹⁴⁹ In the feedback mode, an ultramicroelectrode serves as the SPM tip in an electrochemical cell equipped with a reference electrode and an auxiliary electrode, containing an electroactive species [for example $\text{Fe}(\text{CN})_6^{4-/3-}$ couple, $\text{Ru}(\text{NH}_3)_6^{2+/3+}$ couple] represented as Ox. By adjusting the potential of the tip, using a bi-potentiostat, to a negative value with respect to the reference electrode the electroactive species Ox is reduced at the tip and a Faradaic current flow results, which is influenced by the presence and nature of the investigated sample. The sample can be either conductive or insulating in nature. So when looking at insulating biological samples, the sample is positioned beneath the tip and is not part of the electrode set-up. Scanning the tip over the surface allows for the detection of electroactive species generated at the surface (GC mode). In these first experiments by Bard's laboratory, successful identification of enzymatic activity in mitochondria at the micron level of resolution was achieved.¹³⁷ This technology has been improved by the Kranz and Mizaikoff laboratories where SECM has been combined with AFM by placing an electrode above the contact point on the AFM tip. This allows simultaneous AFM imaging and SECM

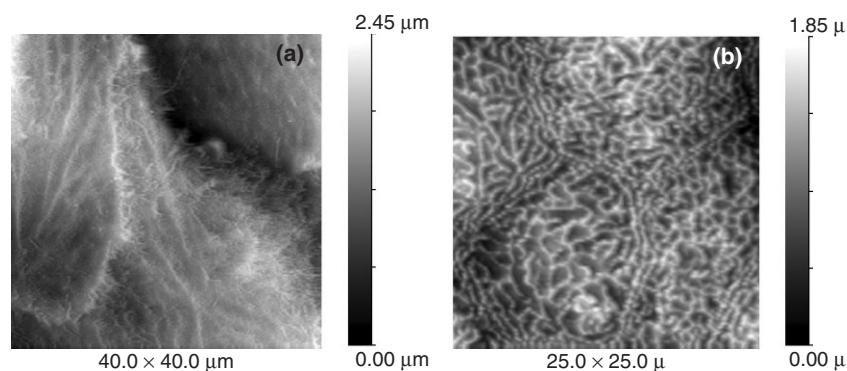


FIGURE 7 | Live cell imaging with scanning ion conductance microscopy (SICM). The image in (A) is an untreated human embryonic cell line NCL-1 imaged in L-15 at room temperature. This unpublished image is provided by Dr Julia Gorelik. (Untreated amphibian kidney epithelial A6 cell line (B) imaged in L-15 at room temperature by Dr. Yuri Korchev.)

imaging in GC or FB mode. In this configuration the electrode is always at the same distance from the surface and lateral resolution of the SECM is improved by the size of the electrode and degree to which the electrode can be placed proximal to the surface.^{150,151} An application of this technique included combining AFM imaging of the enzyme horseradish peroxidase immobilized on gold islands, dispersed on a silicon nitride surface, with the AFM-tip integrated electrode. Following the addition of hydrogen peroxide and hydroxyl methyl ferrocene the SECM recorded images of enzymatic activity occurring on peroxidase immobilized on the gold islands¹⁵² during AFM imaging. In Figure 8 immobilized glucose oxidase at the AFM tip-integrated electrode, demonstrates how a scanning amperometric micro-biosensor for glucose was obtained.¹⁵³

Kelvin probe force microscopy (KPFM) has been integrated into AFM to measure differences in electric potential on surfaces. In the Kelvin method the contact potential difference (CPD) between two surfaces arranged as a parallel plate capacitor is measured. When applied to AFM one plate of the capacitor is the conductive portion of the AFM tip separated by a gap from the other plate of the capacitor that is the sample. By applying an ac bias between the tip and sample a current will flow. The CPD, or with AFM, changes in surface potential, can

be measured by applying a compensating dc voltage to the tip that nullifies the ac field between the tip and sample. During scanning, changes in electrostatic properties of the sample are identified and imaged using a feedback loop that raises or lowers the dc potential to maintain the ac current at zero during scanning. This up/down adjustment of the dc voltage serves as the height input for the KPFM image.¹³⁸ The ability to measure surface potential on biological samples has been reported.^{154–158} Leonenko and co-authors have investigated organization and surface potential of pulmonary surfactant using KPFM in combination with AFM.^{155–157} One of their findings using bovine lipid extract surfactant films, that contain no cholesterol, was that introduction of cholesterol disrupted the assembly of lipid bilayer stacks in the monolayer leading to failure of surfactant function. In the absence of cholesterol, AFM shows the bilayer stacks to be highly structured while the KPFM image shows a potential of up to 200 mV for the large stacks and approximately 100 mV for small stacks.¹⁵⁶ The capability of KPFM to measure electrostatic surface potential of individual biomolecules like DNA and avidin have also been demonstrated, showing that single molecules of negatively charge DNA measured -150 mV and avidin $+10$ mV surface potential compared to the substrate.¹⁵⁸

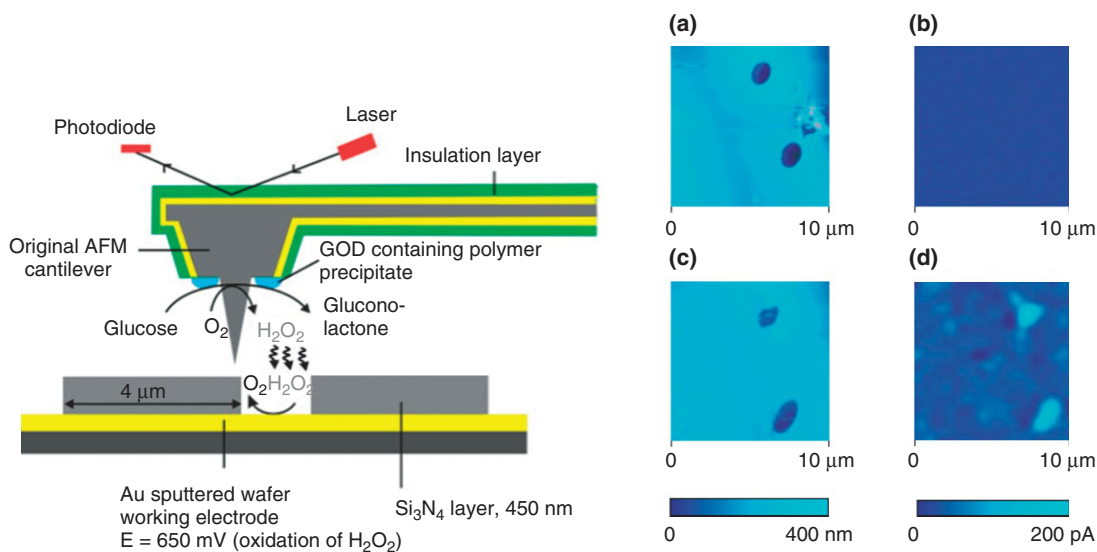


FIGURE 8 | Schematic cross-section of the experimental setup including the reaction scheme of the tip generation/substrate collection mode experiment for imaging glucose with an AFM-tip integrated biosensor (substrate: periodically micropatterned silicon nitride/gold substrate with 1 μm gold electrodes (Quantifoil, Germany)). Simultaneously recorded height (a, c) and current (b, d) current image of glucose conversion with an AFM-tip integrated glucose sensor recorded in AFM contact mode and SECM generator/collector mode. (b) current image in absence of glucose; (d) current image in presence of 3 mM glucose in phosphate buffer pH 7.2. (Courtesy of A. Kueng, B. Mizaiokoff, C. Kranz: unpublished results School of Chemistry and Biochemistry, Georgia Institute of Technology, Atlanta, GA.)

SNFUH is another emerging technique based on AFM imaging. Conventional AFM is limited to imaging surfaces. However, SNFUH has been demonstrated to image structure deep within cells.¹³⁹ This is accomplished by launching a high-frequency acoustic wave (megahertz), that does not interfere with the resonance frequency of the cantilever from beneath the sample. An additional high-frequency acoustic wave (megahertz) of a slightly different frequency is launched from the cantilever with the interference between these two waves forming a surface acoustic standing wave. Perturbations to phase and amplitude of the surface standing wave caused by features buried within the sample are recorded during scanning, via a lock in amplifier, and a SNFUH image is recorded. This technique has allowed simultaneous recording of AFM topographic and SNFUH images of malaria parasites within red blood cells¹³⁹ and nanoparticles within alveolar macrophages.¹⁵⁹

CONCLUSION

In a relatively short period of time, scanning probe microscopes have matured to a point where they

can assume an important role in biological research. AFM is the most commonly used variation. Attributes such as nanometer scale resolution and the ability to operate in liquid environments are in line with key biological imaging requirements. Further, the AFM's range of operation is well suited for characterizing structures from the molecular to cellular scale, and AFM has the unique ability to sensitively measure molecular forces. These features have been exploited for revealing structural detail and for defining the molecular forces involved in a variety of biological systems. In the process of AFM development and adaptation to biological research, instrumentation advances have been plentiful. Higher speed imaging, measurement of electrical characteristics, and molecular identification are just a few of the emerging advances that are facilitating the analysis of various biological structures. The need to understand dynamic biological processes will persist and demand new tools for understanding such processes at the molecular level. Though the application of scanning probe-based tools to this challenge has been brief, they are likely to play an enduring role in biological research.

ACKNOWLEDGEMENTS

The authors acknowledge research support from the US DOE Office of Biological and Environmental Research. Oak Ridge National Laboratory is managed by UT-Battelle, LLC, for the US Department of Energy under Contract no. DEAC05-00OR22725. Ninell P. Mortensen would like to thank Lundbeck Fonden for financial support.

REFERENCES

1. Binnig G, Rohrer H. Scanning tunneling microscopy. *Helv Phys Acta* 1982, 55:726–735.
2. Lindsay SM, Thundat T, Nagahara L, Knipping U, Rill RL. Images of the DNA double helix in water. *Science* 1989, 244:1063–1064.
3. Dunlap DD, Bustamante C. Images of single-stranded nucleic acids by scanning tunnelling microscopy. *Nature* 1989, 342:204–206.
4. Amrein M, Stasiak A, Gross H, Stoll E, Travaglini G. Scanning tunneling microscopy of recA-DNA complexes coated with a conducting film. *Science* 1988, 240:514–516.
5. Lindsay SM, Barris B. Imaging Deoxyribose Nucleic Acid molecules on a metal-surface under water by scanning tunneling microscopy. *J Vac Sci Technol A* 1988, 6:544–547.
6. Beebe TP, Wilson TE, Ogletree DF, Katz JE, Balhorn R, Salmeron MB, Siekhaus WJ. Direct observation of native DNA structures with the scanning tunneling microscope. *Science* 1989, 243:370–372.
7. Allison DP, Bottomley LA, Thundat T, Brown GM, Woychik RP, Schrick JJ, Jacobson KB, Warmack RJ. Immobilization of DNA for scanning probe microscopy. *Proc Natl Acad Sci U S A* 1992, 89:10129–10133.
8. Binnig G, Rohrer H. Scanning tunneling microscopy. In: Janta J, Pantoflicek J, eds. *European Physical Society General Conference*, 6th, Prague, Czechoslovakia, 1984.
9. Dahn DC, Watanabe MO, Blackford BL, Jericho MH, Beveridge TJ. Scanning tunneling microscopy imaging of biological structures. *J Vac Sci Technol A* 1988, 6:548–552.

10. Hameroff S, Simickrstic Y, Verneti L, Lee YC, Sarid D, Wiedmann J, Elings V, Kjoller K, McCuskey R. Scanning tunneling microscopy of cytoskeletal proteins—microtubules and intermediate filaments. *J Vac Sci Technol A* 1990, 8:687–691.
11. Edstrom RD, Meinke MH, Yang X, Yang R, Elings V, Evans DF. Direct visualization of phosphorylase-phosphorylase kinase complexes by scanning tunneling and atomic force microscopy. *Biophys J* 1990, 58:1437–1448.
12. Guckenberger R, Wiegrabe W, Hillebrand A, Hartmann T, Wang ZH, Baumeister W. Scanning tunneling microscopy of a hydrated bacterial surface protein. *Ultramicroscopy* 1989, 31:327–332.
13. Welland ME, Miles MJ, Lambert N, Morris VJ, Coombs JH, Pethica JB. Structure of the globular protein vicilin revealed by scanning tunnelling microscopy. *Int J Biol Macromol* 1989, 11:29–32.
14. Miles MJ, Carr HJ, McMaster TC, PAnson KJ, Belton PS, Morris VJ, Field JM, Shewry PR, Tatham AS. Scanning tunneling microscopy of a wheat seed storage protein reveals details of an unusual supersecondary structure. *Proc Natl Acad Sci U S A* 1991, 88:68–71.
15. Mantovani JG, Allison DP, Warmack RJ, Ferrell TL, Ford JR, Manos RE, Thompson JR, Reddick BB, Jacobson KB. Scanning tunneling microscopy of tobacco mosaic-virus on evaporated and sputter-coated palladium gold substrates. *J Microsc* 1990, 158:109–116.
16. Baro AM, Miranda R, Alaman J, Garcia N, Binnig G, Rohrer H, Gerber C, Carrascosa JL. Determination of surface-topography of biological specimens at high-resolution by scanning tunnelling microscopy. *Nature* 1985, 315:253–254.
17. Binnig G, Quate CF, Gerber C. Atomic force microscope. *Phys Rev Lett* 1986, 56:930–933.
18. Thundat T, Allison DP, Warmack RJ, Ferrell TL. Imaging isolated strands of DNA-molecules by atomic force microscopy. *Ultramicroscopy* 1992, 42:1101–1106.
19. Lindsay SM, Tao NJ, Derosé JA, Oden PI, Lyubchenko YL, Harrington RE, Shlyakhtenko L. Potentiostatic deposition of DNA for scanning probe microscopy. *Biophys J* 1992, 61:1570–1584.
20. Lyubchenko YL, Gall AA, Shlyakhtenko LS, Harrington RE, Jacobs BL, Oden PI, Lindsay SM. Atomic force microscopy imaging of double-stranded DNA and RNA. *J Biomol Struct Dyn* 1992, 10:589–606.
21. Bustamante C, Vesenka J, Tang CL, Rees W, Guthold M, Keller R. Circular DNA-molecules imaged in air by scanning force microscopy. *Biochemistry* 1992, 31:22–26.
22. Hansma PK, Cleveland JP, Radmacher M, Walters DA, Hillner PE, Bezaniilla M, Fritz M, Vie D, Hansma HG, Prater CB, et al. Tapping mode atomic-force microscopy in liquids. *Appl Phys Lett* 1994, 64:1738–1740.
23. Han WH, Lindsay SM, Jing TW. A magnetically driven oscillating probe microscope for operation in liquids. *Appl Phys Lett* 1996, 69:4111–4113.
24. Lantz MA, Oshea SJ, Welland ME. Force microscopy imaging in liquids using Ac techniques. *Appl Phys Lett* 1994, 65:409–411.
25. Lin Y, Wang J, Wan LJ, Fang XH. Study of fibrinogen adsorption on self-assembled monolayers on Au(111) by atomic force microscopy. *Ultramicroscopy* 2005, 105:129–136.
26. Radmacher M, Fritz M, Cleveland JP, Walters DA, Hansma PK. Imaging adhesion forces and elasticity of lysozyme adsorbed on mica with the atomic-force microscope. *Langmuir* 1994, 10:3809–3814.
27. Quist AP, Bjorck LP, Reimann CT, Oscarsson SO, Sundqvist BUR. A scanning force microscopy study of human serum-albumin and porcine pancreas trypsin adsorption on mica surfaces. *Surf Sci* 1995, 325:L406–L412.
28. Hallett P, Offer G, Miles MJ. Atomic-force microscopy of the myosin molecule. *Biophys J* 1995, 68:1604–1606.
29. Hansma HG, Vesenka J, Siegerist C, Kelderman G, Morrett H, Sinsheimer RL, Elings V, Bustamante C, Hansma PK. Reproducible imaging and dissection of plasmid DNA under liquid with the atomic force microscope. *Science* 1992, 256:1180–1184.
30. Henderson E, Haydon PG, Sakaguchi DS. Actin filament dynamics in living glial-cells imaged by atomic force microscopy. *Science* 1992, 257:1944–1946.
31. Radmacher M, Tillmann RW, Fritz M, Gaub HE. From molecules to cells—imaging soft samples with the atomic force microscope. *Science* 1992, 257:1900–1905.
32. Shroff H, Galbraith CG, Galbraith JA, Betzig E. Live-cell photoactivated localization microscopy of nanoscale adhesion dynamics. *Nat Methods* 2008, 5:417–423.
33. Gustafsson MG. Super-resolution light microscopy goes live. *Nat Methods* 2008, 5:385–387.
34. Fernandez-Suarez M, Ting AY. Fluorescent probes for super-resolution imaging in living cells. *Nat Rev Mol Cell Biol* 2008, 9:929–943.
35. Hell SW. Toward fluorescence nanoscopy. *Nat Biotechnol* 2003, 21:1347–1355.
36. Panzer D, Beck C, Maul J, Moller M, Decker H, Schonhense G. Transmission photoemission electron microscopy for lateral mapping of the X-ray absorption structure of a metalloprotein in a liquid cell. *Eur Biophys J* 2008, 38:53–58.

37. de Jonge N, Peckys DB, Kremers GJ, Piston DW. Electron microscopy of whole cells in liquid with nanometer resolution. *Proc Natl Acad Sci U S A* 2009, 106:2159–2164.
38. Hansma HG, Kim KJ, Laney DE, Garcia RA, Argaman M, Allen MJ, Parsons SM. Properties of biomolecules measured from atomic force microscope images: a review. *J Struct Biol* 1997, 119:99–108.
39. Bustamante C, Rivetti C. Visualizing protein-nucleic acid interactions on a large scale with the scanning force microscope. *Annu Rev Biophys Biomol Struct* 1996, 25:395–429.
40. Morris VJ, Kirby AR, Gunning AP. *Atomic Force Microscopy for Biologists*. London: Imperial College Press; 1999.
41. Watanabe Y, Sakurai T. *Advances in Scanning Probe Microscopy*. New York: Springer-Verlag; 2000.
42. Bonnell D. *Scanning Probe Microscopy and Spectroscopy: Theory, Techniques, and Applications*. New York: John Wiley & Sons Inc.; 2000.
43. Muller DJ. AFM: a nanotool in membrane biology. *Biochemistry* 2008, 47:7986–7998.
44. Muller DJ, Helenius J, Alsteens D, Dufrene YF. Force probing surfaces of living cells to molecular resolution. *Nat Chem Biol* 2009, 5:383–390.
45. Puchner EM, Gaub HE. Force and function: probing proteins with AFM-based force spectroscopy. *Curr Opin Struct Biol* 2009, 19:605–614.
46. Giocondi MC, Seantier B, Dosset P, Milhiet PE, Le Grimellec C. Characterizing the interactions between GPI-anchored alkaline phosphatases and membrane domains by AFM. *Pflugers Arch* 2008, 456:179–188.
47. Parot P, Dufrene YF, Hinterdorfer P, Le Grimellec C, Navajas D, Pellequer JL, Scheuring S. Past, present and future of atomic force microscopy in life sciences and medicine. *J Mol Recogn* 2007, 20:418–431.
48. Butt HJ, Wolff EK, Gould SAC, Northern BD, Peterson CM, Hansma PK. Imaging cells with the atomic force microscope. *J Struct Biol* 1990, 105:54–61.
49. Haberle W, Horber JKH, Binnig G. Force microscopy on living cells. *J Vac Sci Technol B* 1991, 9:1210–1213.
50. Haberle W, Horber JKH, Ohnesorge F, Smith DPE, Binnig G. In situ investigations of single living cells infected by viruses. *Ultramicroscopy* 1992, 42:1161–1167.
51. Horber JK, Haberle W, Ohnesorge F, Binnig G, Liebich HG, Czerny CP, Mahnel H, Mayr A. Investigation of living cells in the nanometer regime with the scanning force microscope. *Scanning Microsc* 1992, 6:919–929; discussion 929–930.
52. Hoh JH, Schoenberger CA. Surface-morphology and mechanical-properties of Mdkc monolayers by atomic-force microscopy. *J Cell Sci* 1994, 107:1105–1114.
53. Fritz M, Radmacher M, Gaub HE. Granula motion and membrane spreading during activation of human platelets imaged by atomic-force microscopy. *Biophys J* 1994, 66:1328–1334.
54. Le Grimellec C, Lesniewska E, Cachia C, Schreiber JP, Defornel F, Goudonnet JP. Imaging of the membrane-surface of Mdkc cells by atomic-force microscopy. *Biophys J* 1994, 67:36–41.
55. Kasas S, Ikai A. A method for anchoring round shaped cells for atomic-force microscope imaging. *Biophys J* 1995, 68:1678–1680.
56. Dufrene YF, Boonaert CJP, Gerin PA, Asther M, Rouxhet PG. Direct probing of the surface ultrastructure and molecular interactions of dormant and germinating spores of *Phanerochaete chrysosporium*. *J Bacteriol* 1999, 181:5350–5354.
57. Touhami A, Jericho MH, Beveridge TJ. Atomic force microscopy of cell growth and division in *Staphylococcus aureus*. *J Bacteriol* 2004, 186:3286–3295.
58. van der Mei HC, Busscher HJ, Bos R, de Vries J, Boonaert CJP, Dufrene YF. Direct probing by atomic force microscopy of the cell surface softness of a fibrillated and nonfibrillated oral streptococcal strain. *Biophys J* 2000, 78:2668–2674.
59. Francius G, Domenech O, Mingeot-Leclercq MP, Dufrene YF. Direct observation of *staphylococcus aureus* cell wall digestion by lysostaphin. *J Bacteriol* 2008, 190:7904–7909.
60. Mendez-Vilas A, Gallardo-Moreno AM, Gonzalez-Martin ML. Atomic force microscopy of mechanically trapped bacterial cells. *Microsc Microanal* 2007, 13:55–64.
61. Beckmann MA, Venkataraman S, Doktycz MJ, Nataro JP, Sullivan CJ, Morrell-Falvey JL, Allison DP. Measuring cell surface elasticity on enteroaggregative *Escherichia coli* wild type and dispersin mutant by AFM. *Ultramicroscopy* 2006, 106:695–702.
62. Mortensen NP, Fowlkes JD, Sullivan CJ, Allison DP, Larsen NB, Molin S, Doktycz MJ. Effects of colistin on surface ultrastructure and nanomechanics of *Pseudomonas aeruginosa* cells. *Langmuir* 2009, 25:3728–3733.
63. Sullivan CJ, Venkataraman S, Retterer ST, Allison DP, Doktycz MJ. Comparison of the indentation and elasticity of *E-coli* and its spheroplasts by AFM. *Ultramicroscopy* 2007, 107:934–942.
64. Shu AC, Wu CC, Chen YY, Peng HL, Chang HY, Yew TR. Evidence of DNA transfer through F-pilus channels during *Escherichia coli* conjugation. *Langmuir* 2008, 24:6796–6802.
65. Arce FT, Carlson R, Monds J, Veeh R, Hu FZ, Stewart PS, Lal R, Ehrlich GD, Avci R. Nanoscale structural and mechanical properties of nontypeable

- haemophilus influenzae biofilms. *J Bacteriol* 2009, 191:2512–2520.
66. Plomp M, Leighton TJ, Wheeler KE, Hill HD, Malkin AJ. In vitro high-resolution structural dynamics of single germinating bacterial spores. *Proc Natl Acad Sci U S A* 2007, 104:9644–9649.
67. Doktycz MJ, Sullivan CJ, Hoyt PR, Pelletier DA, Wu S, Allison DP. AFM imaging of bacteria in liquid media immobilized on gelatin coated mica surfaces. *Ultramicroscopy* 2003, 97:209–216.
68. Schoenenberger CA, Hoh JH. Slow cellular-dynamics in Mdkc and R5 cells monitored by time-lapse atomic-force microscopy. *Biophys J* 1994, 67:929–936.
69. Weisenhorn AL, Khosandi M, Kasas S, Gotzos V, Butt HJ. Deformation and height anomaly of soft surfaces studied with an AFM. *Nanotechnology* 1993, 4:106–113.
70. Radmacher M, Fritz M, Hansma PK. Imaging soft samples with the atomic-force microscope—gelatin in water and propanol. *Biophys J* 1995, 69:264–270.
71. Radmacher M. Measuring the elastic properties of biological samples with the AFM. *IEEE Eng Med Biol Mag* 1997, 16:47–57.
72. Le Grimmelc C, Lesniewska E, Giocondi MC, Finot E, Vie V, Goudonnet JP. Imaging of the surface of living cells by low-force contact-mode atomic force microscopy. *Biophys J* 1998, 75:695–703.
73. Lesniewska E, Giocondi MC, Vie V, Finot E, Goudonnet JP, Le Grimmelc C. Atomic force microscopy of renal cells: limits and prospects. *Kidney Int* 1998, 53(Supp 65), S42–S48.
74. Parpura V, Haydon PG, Henderson E. 3-Dimensional imaging of living neurons and Glia with the atomic force microscope. *J Cell Sci* 1993, 104:427–432.
75. You HX, Yu L. Atomic force microscopy imaging of living cells: progress, problems and prospects. *Methods Cell Sci* 1999, 21:1–17.
76. Vie V, Giocondi MC, Lesniewska E, Finot E, Goudonnet JP, Le Grimmelc C. Tapping-mode atomic force microscopy on intact cells: optimal adjustment of tapping conditions by using the deflection signal. *Ultramicroscopy* 2000, 82:279–288.
77. Lucius H, Friedrichson T, Kurzchalia TV, Lewin GR. Identification of caveolae-like structures on the surface of intact cells using scanning force microscopy. *J Membr Biol* 2003, 194:97–108.
78. Nagao E, Dvorak JA. An integrated approach to the study of living cells by atomic force microscopy. *J Microsc* 1998, 191:8–19.
79. Le Grimmelc C, Giocondi MC, Lenoir M, Vater M, Sposito G, Pujol R. High-resolution three-dimensional imaging of the lateral plasma membrane of cochlear outer hair cells by atomic force microscopy. *J Comp Neurol* 2002, 451:62–69.
80. Hoh JH, Cleveland JP, Prater CB, Revel JP, Hansma PK. Quantized adhesion detected with the atomic force microscope. *J Am Chem Soc* 1992, 114:4917–4918.
81. Goldmann WH, Galneder R, Ludwig M, Xu WM, Adamson ED, Wang N, Ezzell RM. Differences in elasticity of vinculin-deficient F9 cells measured by magnetometry and atomic force microscopy. *Exp Cell Res* 1998, 239:235–242.
82. Yao X, Jericho M, Pink D, Beveridge T. Thickness and elasticity of gram-negative murein sacculi measured by atomic force microscopy. *J Bacteriol* 1999, 181:6865–6875.
83. Yao X, Walter J, Burke S, Stewart S, Jericho MH, Pink D, Hunter R, Beveridge TJ. Atomic force microscopy and theoretical considerations of surface properties and turgor pressures of bacteria. *Colloids Surf B Biointerfaces* 2002, 23:213–230.
84. Velegol SB, Logan BE. Contributions of bacterial surface polymers, electrostatics, and cell elasticity to the shape of AFM force curves. *Langmuir* 2002, 18:5256–5262.
85. Arnoldi M, Fritz M, Bauerlein E, Radmacher M, Sackmann E, Boulbitch A. Bacterial turgor pressure can be measured by atomic force microscopy. *Phys Rev E* 2000, 62:1034–1044.
86. Gaboriaud F, Baillet S, Dague E, Jorand F. Surface structure and nanomechanical properties of *Shewanella putrefaciens* bacteria at two pH values (4 and 10) determined by atomic force microscopy. *J Bacteriol* 2005, 187:3864–3868.
87. Gaboriaud F, Dufrene YF. Atomic force microscopy of microbial cells: application to nanomechanical properties, surface forces and molecular recognition forces. *Colloids Surf B Biointerfaces* 2007, 54:10–19.
88. Pelling AE, Li YN, Shi WY, Gimzewski JK. Nanoscale visualization and characterization of *Myxococcus xanthus* cells with atomic force microscopy. *Proc Natl Acad Sci U S A* 2005, 102:6484–6489.
89. Cerf A, Cau JC, Vieu C, Dague E. Nanomechanical properties of dead or alive single-patterned bacteria. *Langmuir* 2009, 25:5731–5736.
90. Charras GT, Horton MA. Single cell mechanotransduction and its modulation analyzed by atomic force microscope indentation. *Biophys J* 2002, 82:2970–2981.
91. A-Hassan E, Heinz WF, Antonik MD, D'Costa NP, Nageswaran S, Schoenenberger CA, Hoh JH. Relative microelastic mapping of living cells by atomic force microscopy. *Biophys J* 1998, 74:1564–1578.
92. Schmitz J, Benoit M, Gottschalk KE. The viscoelasticity of membrane tethers and its importance for cell adhesion. *Biophys J* 2008, 95:1448–1459.
93. Matzke R, Jacobson K, Radmacher M. Direct, high-resolution measurement of furrow stiffening during division of adherent cells. *Nat Cell Biol* 2001, 3:607–610.

94. Birukova AA, Arce FT, Moldobaeva N, Dudek SM, Garcia JG, Lal R, Birukov KG. Endothelial permeability is controlled by spatially defined cytoskeletal mechanics: atomic force microscopy force mapping of pulmonary endothelial monolayer. *Nanomedicine* 2009, 5:30–41.
95. Roduit C, van der Goot FG, De Los Rios P, Yersin A, Steiner P, Dietler G, Catsicas S, Lafont F, Kasas S. Elastic membrane heterogeneity of living cells revealed by stiff nanoscale membrane domains. *Biophys J* 2008, 94:1521–1532.
96. Mathur AB, Collinworth AM, Reichert WM, Kraus WE, Truskey GA. Endothelial, cardiac muscle and skeletal muscle exhibit different viscous and elastic properties as determined by atomic force microscopy. *J Biomech* 2001, 34:1545–1553.
97. Takai E, Costa KD, Shaheen A, Hung CT, Guo XE. Osteoblast elastic modulus measured by atomic force microscopy is substrate dependent. *Ann Biomed Eng* 2005, 33:963–971.
98. Boland T, Ratner BD. Direct measurement of hydrogen bonding in DNA nucleotide bases by atomic force microscopy. *Proc Natl Acad Sci U S A* 1995, 92:5297–5301.
99. Lee GU, Chrisey LA, Colton RJ. Direct measurement of the forces between complementary strands of DNA. *Science* 1994, 266:771–773.
100. Florin EL, Moy VT, Gaub HE. Adhesion forces between individual ligand-receptor pairs. *Science* 1994, 264:415–417.
101. Moy VT, Florin EL, Gaub HE. Intermolecular forces and energies between ligands and receptors. *Science* 1994, 266:257–259.
102. Lee GU, Kidwell DA, Colton RJ. Sensing discrete streptavidin biotin interactions with atomic-force microscopy. *Langmuir* 1994, 10:354–357.
103. Benoit M, Gabriel D, Gerisch G, Gaub HE. Discrete interactions in cell adhesion measured by single-molecule force spectroscopy. *Nat Cell Biol* 2000, 2:313–317.
104. Han T, Williams JM, Beebe TP. Chemical-bonds studied with functionalized atomic-force microscopy tips. *Anal Chim Acta* 1995, 307:365–376.
105. Rief M, Gautel M, Oesterhelt F, Fernandez JM, Gaub HE. Reversible unfolding of individual titin immunoglobulin domains by AFM. *Science* 1997, 276:1109–1112.
106. Marszalek PE, Lu H, Li H, Carrion-Vazquez M, Oberhauser AF, Schulten K, Fernandez JM. Mechanical unfolding intermediates in titin modules. *Nature* 1999, 402:100–103.
107. Tskhovrebova L, Trinick J. Extensibility in the titin molecule and its relation to muscle elasticity. *Adv Exp Med Biol* 2000, 481:163–173; discussion 174–178.
108. Oberhauser AF, Marszalek PE, Erickson HP, Fernandez JM. The molecular elasticity of the extracellular matrix protein tenascin. *Nature* 1998, 393:181–185.
109. Muller DJ, Baumeister W, Engel A. Controlled unzipping of a bacterial surface layer with atomic force microscopy. *Proc Natl Acad Sci U S A* 1999, 96:13170–13174.
110. Li HB, Rief M, Oesterhelt F, Gaub HE, Zhang X, Shen JC. Single-molecule force spectroscopy on polysaccharides by AFM—nanomechanical fingerprint of alpha-(1,4)-linked polysaccharides. *Chem Phys Lett* 1999, 305:197–201.
111. Li HB, Zhang WK, Xu WQ, Zhang X. Hydrogen bonding governs the elastic properties of poly(vinyl alcohol) in water: Single-molecule force spectroscopic studies of PVA by AFM. *Macromolecules* 2000, 33:465–469.
112. Wildling L, Hinterdorfer P, Kusche-Vihrog K, Treffner Y, Oberleithner H. Aldosterone receptor sites on plasma membrane of human vascular endothelium detected by a mechanical nanosensor. *Pflugers Arch* 2009, 458:223–230.
113. Gad M, Itoh A, Ikai A. Mapping cell wall polysaccharides of living microbial cells using atomic force microscopy. *Cell Biol Int* 1997, 21:697–706.
114. Grandbois M, Dettmann W, Benoit M, Gaub HE. Affinity imaging of red blood cells using an atomic force microscope. *J Histochem Cytochem* 2000, 48:719–724.
115. Jiang YX, Wang J, Fang XH, Bai CL. Study of the effect of metal ion on the specific interaction between protein and aptamer by atomic force microscopy. *J Nanosci Nanotechnol* 2004, 4:611–615.
116. Dupres V, Menozzi FD, Loch C, Clare BH, Abbott NL, Cuenot S, Bompard C, Raze D, Dufrene YF. Nanoscale mapping and functional analysis of individual adhesins on living bacteria. *Nat Methods* 2005, 2:515–520.
117. Alsteens D, Dague E, Rouxhet PG, Baulard AR, Dufrene YF. Direct measurement of hydrophobic forces on cell surfaces using AFM. *Langmuir* 2007, 23:11977–11979.
118. Touhami A, Hoffmann B, Vasella A, Denis FA, Dufrene YF. Aggregation of yeast cells: direct measurement of discrete lectin-carbohydrate interactions. *Microbiology* 2003, 149:2873–2878.
119. Gilbert Y, Deghorain M, Wang L, Xu B, Pollheimer PD, Gruber HJ, Errington J, Hallet B, Haulot X, Verbelen C, et al. Single-molecule force spectroscopy and imaging of the vancomycin/D-Ala-D-Ala interaction. *Nano Lett* 2007, 7:796–801.
120. Pfister G, Stroh CM, Perschinka H, Kind M, Knoflach M, Hinterdorfer P, Wick G. Detection of HSP60 on the membrane surface of stressed human

- endothelial cells by atomic force and confocal microscopy. *J Cell Sci* 2005, 118:1587–1594.
121. Wojcikiewicz EP, Abdulreda MH, Zhang X, Moy VT. Force spectroscopy of LFA-1 and its ligands, ICAM-1 and ICAM-2. *Biomacromolecules* 2006, 7:3188–3195.
122. Chtcheglova LA, Waschke J, Wildling L, Drenckhahn D, Hinterdorfer P. Nano-scale dynamic recognition imaging on vascular endothelial cells. *Biophys J* 2007, 93:L11–L13.
123. Almqvist N, Bhatia R, Primbs G, Desai N, Banerjee S, Lal R. Elasticity and adhesion force mapping reveals real-time clustering of growth factor receptors and associated changes in local cellular rheological properties. *Biophys J* 2004, 86:1753–1762.
124. Lehenkari PP, Charras GT, Nykanen A, Horton MA. Adapting atomic force microscopy for cell biology. *Ultramicroscopy* 2000, 82:289–295.
125. Raab A, Han WH, Badt D, Smith-Gill SJ, Lindsay SM, Schindler H, Hinterdorfer P. Antibody recognition imaging by force microscopy. *Nat Biotechnol* 1999, 17:902–905.
126. Stroh CM, Ebner A, Geretschlager M, Freudenthaler G, Kienberger F, Kamruzzahan ASM, Smith-Gil SJ, Gruber HJ, Hinterdorfer P. Simultaneous topography and recognition Imaging using force microscopy. *Biophys J* 2004, 87:1981–1990.
127. Hansma HG, Laney DE. DNA binding to mica correlates with cationic radius: assay by atomic force microscopy. *Biophys J* 1996, 70:1933–1939.
128. Thomson NH, Fritz M, Radmacher M, Cleveland JP, Schmidt CF, Hansma PK. Protein tracking and detection of protein motion using atomic force microscopy. *Biophys J* 1996, 70:2421–2431.
129. Kasas S, Thomson NH, Smith BL, Hansma HG, Zhu X, Guthold M, Bustamante C, Kool ET, Kashlev M, Hansma PK. Escherichia coli RNA polymerase activity observed using atomic force microscopy. *Biochemistry* 1997, 36:461–468.
130. Radmacher M, Fritz M, Hansma HG, Hansma PK. Direct observation of enzyme-activity with the atomic-force microscope. *Science* 1994, 265:1577–1579.
131. Wang H, Bash R, Yodh JG, Hager G, Lindsay SM, Lohr D. Using atomic force microscopy to study nucleosome remodeling on individual nucleosomal arrays in situ. *Biophys J* 2004, 87:1964–1971.
132. Rotsch C, Radmacher M. Drug-induced changes of cytoskeletal structure and mechanics in fibroblasts: an atomic force microscopy study. *Biophys J* 2000, 78:520–535.
133. Ohnesorge FM, Horber JKH, Haberle W, Czerny CP, Smith DPE, Binnig G. AFM review study on pox viruses and living cells. *Biophys J* 1997, 73:2183–2194.
134. Schneider SW, Sritharan KC, Geibel JP, Oberleithner H, Jena BP. Surface dynamics in living acinar cells imaged by atomic force microscopy: Identification of plasma membrane structures involved in exocytosis. *Proc Natl Acad Sci U S A* 1997, 94:316–321.
135. Ando T, Kodera N, Takai E, Maruyama D, Saito K, Toda A. A high-speed atomic force microscope for studying biological macromolecules. *Proc Natl Acad Sci U S A* 2001, 98:12468–12472.
136. Hansma PK, Drake B, Marti O, Gould SAC, Prater CB. The scanning ion-conductance microscope. *Science* 1989, 243:641–643.
137. Bard AJ, Fan FRF, Pierce DT, Unwin PR, Wipf DO, Zhou FM. Chemical imaging of surfaces with the scanning electrochemical microscope. *Science* 1991, 254:68–74.
138. Nonnenmacher M, Oboyle MP, Wickramasinghe HK. Kelvin probe force microscopy. *Appl Phys Lett* 1991, 58:2921–2923.
139. Shekhawat GS, Dravid VP. Nanoscale imaging of buried structures via scanning near-field ultrasound holography. *Science* 2005, 310:89–92.
140. Casuso I, Kodera N, Le Grimmelc C, Ando T, Scheuring S. Contact-mode high-resolution high-speed atomic force microscopy movies of the purple membrane. *Biophys J* 2009, 97:1354–1361.
141. Picco LM, Dunton PG, Ulcinas A, Engledew DJ, Hoshi O, Ushiki T, Miles MJ. High-speed AFM of human chromosomes in liquid. *Nanotechnology* 2008, 19.
142. Fantner GE, Schitter G, Kindt JH, Ivanov T, Ivanova K, Patel R, Holtén-Andersen N, Adams J, Thurner PJ, Rangelow IW, et al. Components for high speed atomic force microscopy. *Ultramicroscopy* 2006, 106:881–887.
143. Humphris ADL, Miles MJ, Hobbs JK. A mechanical microscope: high-speed atomic force microscopy. *Appl Phys Lett* 2005, 86.
144. Proksch R, Lal R, Hansma PK, Morse D, Stucky G. Imaging the internal and external pore structure of membranes in fluid: tappingmode scanning ion conductance microscopy. *Biophys J* 1996, 71:2155–2157.
145. Korchev YE, Bashford CL, Milovanovic M, Vodyanoy I, Lab MJ. Scanning ion conductance microscopy of living cells. *Biophys J* 1997, 73:653–658.
146. Shevchuk AI, Frolenkov GI, Sanchez D, James PS, Freedman N, Lab MJ, Jones R, Klenerman D, Korchev YE. Imaging proteins in membranes of living cells by high-resolution scanning ion conductance microscopy. *Angew Chem Int Ed Engl* 2006, 45:2212–2216.
147. Novak P, Li C, Shevchuk AI, Stepanyan R, Caldwell M, Hughes S, Smart TG, Gorelik J, Ostanin VP, Lab MJ, et al. Nanoscale live-cell imaging using hopping probe ion conductance microscopy. *Nat Methods* 2009, 6:279–281.

148. Lee C, Kwak JY, Anson FC. Application of scanning electrochemical microscopy to generation/collection experiments with high collection efficiency. *Anal Chem* 1991, 63:1501–1504.
149. Kwak J, Bard AJ. Scanning electrochemical microscopy—theory of the feedback mode. *Anal Chem* 1989, 61:1221–1227.
150. Wiedemair J, Balu B, Moon JS, Hess DW, Mizaikoff B, Kranz C. Plasma-deposited fluorocarbon films: insulation material for microelectrodes and combined atomic force microscopy-scanning electrochemical microscopy probes. *Anal Chem* 2008, 80:5260–5265.
151. Kranz C, Friedbacher G, Mizaikoff B, Lugstein A, Smoliner J, Bertagnolli E. Integrating an ultramicroelectrode in an AFM cantilever: combined technology for enhanced information. *Anal Chem* 2001, 73:2491–2500.
152. Kranz C, Kueng A, Lugstein A, Bertagnolli E, Mizaikoff B. Mapping of enzyme activity by detection of enzymatic products during AFM imaging with integrated SECM-AFM probes. *Ultramicroscopy* 2004, 100:127–134.
153. Kueng A, Kranz C, Mizaikoff B, Lugstein A, Bertagnolli E, Mizaikoff B. AFM-tip integrated amperometric biosensors: high resolution imaging of membrane transport. *Angew Chem Int Ed* 2005, 44:3419–3422.
154. Kwak KJ, Yoda S, Fujihira M. Observation of stretched single DNA molecules by Kelvin probe force microscopy. *Appl Surf Sci* 2003, 210:73–78.
155. Hane F, Moores B, Amrein M, Leonenko Z. Effect of SP-C on surface potential distribution in pulmonary surfactant: atomic force microscopy and Kelvin probe force microscopy study. *Ultramicroscopy* 2009, 109:968–973.
156. Leonenko Z, Gill S, Baoukina S, Monticelli L, Doehner J, Gunasekara L, Felderer F, Rodenstein M, Eng LM, Amrein M. An elevated level of cholesterol impairs self-assembly of pulmonary surfactant into a functional film. *Biophys J* 2007, 93:674–683.
157. Leonenko Z, Rodenstein M, Dohner J, Eng LM, Amrein M. Electrical surface potential of pulmonary surfactant. *Langmuir* 2006, 22:10135–10139.
158. Leung C, Kinns H, Hoogenboom BW, Howorka S, Mesquida P. Imaging surface charges of individual biomolecules. *Nano Lett* 2009, 9:2769–2773.
159. Tetard L, Passian A, Venmar KT, Lynch RM, Voy BH, Shekhawat G, Dravid VP, Thundat T. Imaging nanoparticles in cells by nanomechanical holography. *Nat Nanotechnol* 2008, 3:501–505.